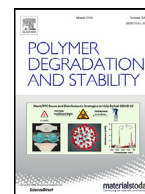




Contents lists available at ScienceDirect

Polymer Degradation and Stability

journal homepage: www.elsevier.com/locate/polymdegradstab

Kinetic Study of Paper Waste Thermal Degradation

Zhuo Xu^a, Shreyas S. Kolapkar^a, Stas Zinchik^a, Ezra Bar-Ziv^{a,*}, Jordan Klinger^b,
Eric Fillerup^b, Kastli Schaller^b, Corey Pilgrim^c

^a Michigan Technological University, 1400 Townsend Dr, Houghton, MI 49931, United States

^b Energy & Environment S&T, Idaho National Laboratory, 1955 N. Fremont Avenue, Idaho Falls, Idaho 83415, United States

^c Nuclear Science and Technology, Idaho National Laboratory, 1955 N. Fremont Avenue, Idaho Falls, Idaho 83415, United States

ARTICLE INFO

Article history:

Received 1 April 2021

Revised 5 July 2021

Accepted 14 July 2021

Available online 18 July 2021

Keywords:

Kinetics

Paper waste

TGA

Thermal degradation

NMR spectroscopy

ABSTRACT

Paper waste generation has been rising in the past decades, with a large amount being landfilled. These paper wastes can be great energy sources after thermal treatment since they are considered carbon neutral. These wastes contain mainly cellulose, hemicellulose, lignin, and some minerals. The thermal decomposition of cellulose, hemicellulose, and lignin have been extensively studied, however, the knowledge of thermal degradation of paper wastes at lower temperatures, which are more practical for industrial applications are still lacking. In this study, paper wastes have been characterized and thermogravimetric analyses were performed from 200°C to 400°C and the char produced were analyzed by nuclear magnetic resonance (NMR) spectroscopy and Fourier-transform infrared (FTIR) spectroscopy. Two kinetic approaches were taken while developing the kinetic model of paper waste thermal degradation: (i) reconstructing the TGA results of paper waste thermal degradation by an additive law of the degradation of cellulose, hemicellulose and lignin; (ii) considering paper waste as one material and develop a multi-step consecutive reaction mechanism that focuses on solid products at different temperatures. It was observed that there are potential interactions between cellulose, hemicellulose and lignin during paper waste degradation. Therefore, the second approach was concluded to be more plausible, and one set of kinetic parameters were determined according to the experimental results at different temperatures. These results provided insights into the degradation kinetic mechanism and solid product distribution of the paper waste. It was found that the first reaction was due to dehydration of cellulose and the 6th and 7th reaction can be attributed to the thermal degradation of lignin. The NMR and FTIR results also validated that the cellulose started degrading at lower temperatures, and lignin degradation became more pronounced at higher temperatures.

© 2021 Elsevier Ltd. All rights reserved.

1. Introduction

Waste generation across the globe has been rising, and paper waste is one of the major contributors to this growth. For instance, U.S. alone produced about 67 million tons of paper waste in 2017, with 18.4 million tons been landfilled [1]. These landfilled paper wastes are usually mixed with different materials, which makes them economically prohibitive to recycle. The landfill approach is not only inefficient in utilizing resources, but it would also produce greenhouse gases during the decomposition process. A potential alternative is treating these non-recyclable wastes with a thermal process and turn them into energy sources, which has been proven to be carbon-neutral [2].

The paper wastes used in this study mainly consists of used paper and cardboard, which contain mostly cellulose, with lower level of hemicellulose, lignin, and inorganic material analyzed as ash content [3,4]. In order to study the thermal degradation of paper, it is essential to understand the behavior of cellulose, hemicellulose, and lignin during thermal degradation. The following provides a review of the kinetics of thermal degradation of cellulose hemicellulose and lignin. Since cellulose hemicellulose and lignin have been extensively studied by many researchers, we restricted our review to a few studies.

Bradbury et al., proposed a mechanism for cellulose thermal degradation (Broido-Shafizadeh mechanism) [5]. The mechanism suggests that the cellulose first produces active cellulose, during which the cellulose does not lose any mass. This reaction will subsequently go through two pathways, with one reaction producing volatiles, another decomposing into char and gases.

* Corresponding author.

E-mail address: ebarziv@mtu.edu (E. Bar-Ziv).

Cabrales and Abidi have studied the thermal degradation of cellulose of cotton fibers [6]. Reaction rate was calculated by the Arrhenius equation and activation energy was modeled as a function of the conversion level. It was stated that the thermal degradation of cellulose was a multi-step process, and the results showed that this process was governed by the slowest. Mamleev et al., studied the kinetics of cellulose thermal decomposition and focused on the main step of mass loss [7]. A two-step reaction mechanism was proposed, and the kinetic parameters were obtained; this study focused on 300°C.

The hemicellulose thermal degradation was also well investigated in the literature [8,9]. The studies included different steps and product distributions during the degradation process. It was also found that hemicellulose is easier to degrade compared to cellulose. Hemicellulose produced more CO₂, which can be attributed to its higher carboxyl content; and cellulose had higher CO yield, due to the existence of carboxyl and carbonyl.

The lignin decomposes slower at the studied temperature range (200°C–400°C) in comparison to cellulose and hemicellulose [10]. It has been found that lignin thermal degradation has two reaction rate peaks below 400°C. The first one is at the range of 100–180°C, due to the elimination of moisture, and the second from 375–400°C. In addition, the reactions at around 400°C produce mainly aromatic hydrocarbons, such as hydroxy phenolics and phenolics [11,12]. These studies shed some light on the products of the lignin thermal degradation.

Although the thermal degradation of cellulose, hemicellulose and lignin has been well documented, the existence of interactions between the three components in mixtures has been controversial. Some researchers did not observe interactions between cellulose and lignin during thermal degradation [11,13–15], while others reported notable interactions [16–19]. Zhang et al., studied the interactions between native (plant biomass) and non-native (physical mixture) cellulose-hemicellulose mixture and cellulose-lignin mixture [20]. They found that there are no significant interactions between the physical mixture of cellulose-lignin, cellulose-hemicellulose and woody native cellulose-lignin samples. However, the interactions were observed in native cellulose–lignin mixture, as the levoglucosan yield decreased and the low molecular weight compounds and furans yield increased. Recently, Yang et al., found that the volatiles produced from hemicellulose at 280°C could interact with cellulose and lignin and promote their decomposition [21]. In addition, it was observed that the volatiles produced from cellulose at 315°C were captured by lignin to form aromatic rings. There are other studies that are not reviewed here, however, they further emphasized the controversy of existence of interactions between the three components. In order to understand paper waste degradation at the temperature range of 225°C–400°C, it is essential to study if there are potential interactions between cellulose, hemicellulose and lignin that are the main constituents in papers. If there are no interactions, paper degradation can be described by a simple additive rule of the three components. If there are such interactions during thermal degradation, paper wastes should be treated as one material, such as done in kinetics of biomass (that is also mainly consist of cellulose, hemicellulose and lignin) degradation at these temperatures; for example, see references [22–25] and references cited therein.

Although both biomass and paper wastes mainly consist of cellulose, hemicellulose and lignin, the two material have different chemical structures. For example, the cellulose in the biomass is usually a relatively long thread that is the main structural material which formed plant cell wall [26]. However, during paper making processes, especially pulping, drying and printing, the structure of cellulosic fibers can undergo significant changes [27]. Further, paper wastes also contains various chemical additives [28].

In this paper, we present comprehensive study of paper thermal degradation in the temperature range of 225°C to 400°C, that comprises experimental TGA measurements of paper waste and the individual cellulose, hemicellulose and lignin components. We attempted to analyze and interpret the experimental results by two kinetic approaches: (i) reconstructing the TGA results of paper waste thermal degradation by an additive law of the degradation of cellulose, hemicellulose and lignin; (ii) consider paper waste as one material to develop the model. It was found that there are potential interactions between cellulose, hemicellulose and lignin during paper degradation. Therefore, we took second approach mentioned above.

Biomass thermal degradation models have been well-documented in the literature. Different mechanisms were investigated, including parallel reactions [29–32], and consecutive reaction mechanisms [22,33–35]. Since interactions were observed between cellulose, hemicellulose and lignin from both paper waste and biomass, the biomass thermal degradation model could be adopted to study the paper waste degradation. This paper adopted the commonly used consecutive reaction mechanism [22,36–38] that focuses on solid products at different temperatures. This approach can both provide more insights in paper wastes thermal degradation and can effectively help to design paper waste thermal treating processes for the industrial systems.

2. Material and methods

2.1. Material

The materials used in this study were non-recyclable industrial paper waste, and commercially available cellulose powder (Avicel PH-101, Fluka), hemicellulose (extracted xylan from corncob, Carbosynth), and lignin (Sigma Aldrich, 471054). The paper waste consists of paper, cardboard, carton, wax papers and laminated paper residuals. Details of the paper waste has been covered in the previous work [39,40]. The paper wastes went through three stages of downsizing and the final size is 2 by 2 mm sized to reduce heterogeneity of the original material. No additional treatment was performed for the commercial cellulose, hemicellulose, and lignin.

2.2. Experimental methods

2.2.1. Thermal properties analysis

Thermal conductivity was measured by ThermTest Inc. TPS15000. The samples are placed in an oven and two multi-meters with 100nV accuracy were used. The results were analyzed with a custom build Virtual Instrument in Labview. As the interface temperature changes, the sample thermal diffusivity is fitted to match changes in resistance. The voltage potential across the sensor was used to calculate the sensor transient resistance. More details were provided in the previous work [41].

2.2.2. Molecular weight

Waste paper and Avicel®PH 101 were characterized for molecular weight distributions as described in previous work [42]. The materials were prepared for molecular weight analysis using N, N-dimethylacetamide (HPLC grade, Sigma-Aldrich) and lithium chloride (99.9% Bioextra, Sigma-Aldrich) as solvents after fine milling the solids to less than 200 microns. The molecular weight distribution was determined using an Agilent 1200 HPLC (Agilent Technologies Inc., Santa Clara, CA) with a refractive index detector. Chromatographic conditions were: 2 in-line PLgel 20µm Mixed-A LS 300×7.5 mm columns and guard column; refractive index detector temperature 35°C; column temperature 70°C; 0.5% LiCl in N,N-dimethylacetamide mobile phase at a flow rate of 1.0mL/min.

Cellulose standards (Pullulan standards, Agilent) of varying molecular weight from 180 to 640,000 g/mol were prepared in the same mobile phase and were used to calibrate the column and compared to retention times of samples. From this calibration, the retention times and retention time distributions of the primary eluent peaks indicated the molecular weight distribution of the solids.

2.2.3. Thermogravimetric analysis (TGA)

A LECO TGA 701 was used to carry out thermogravimetric analysis. The balance in the instrument measures the weight of the sample during the experiments. When the oven temperature reaches 110°C, the moisture started to release, and the weight of the material started reducing. The temperature of the oven is kept at 110°C until the weight stopped dropping to eliminate all the moisture in the sample. The temperature will then increase to the set temperature with 16°C/min (highest heating rate for this instrument). The sample mass was measured by a balance with 0.0001g readability.

2.2.4. Solid-state $^{13}\text{C}\{^1\text{H}\}$ -CP/MAS NMR and FTIR spectroscopy

10 wt% of adamantane was mixed with solid samples to as a reference since the temperature significantly affects the densities of carbon species. The paper/adamantane mixtures were ground to produce homogeneous particles. A Bruker Avance III spectrometer with a field strength of 9.4 T was used to gather the spectra with a magic-angle spinning (MAS) probe. The samples spun at 15 kHz and these experiments used standard cross-polarization (CP) experiment [43,44]. For each individual sample, ^1H NMR spectra were recorded to determine the center of the excitation profile for the CP experiment.

Conditions for the cross-polarization experiment were optimized on a highly torrefied sample first (325°C), to ensure that the conditions provided quantitation for the broad peak seen growing in. The contact time of the CP pulse program was set to 1.8 msec and the nutation frequency was set at 92.6 kHz. SPINAL64 decoupling was used with a field strength of 48.0 kHz [45]. The final parameters of the experiment included a sweep width of 745 ppm, a longitudinal relaxation delay of 4 sec, and the total number of scans set to 3072. Only 900 points of the total 4004 experimental points in the free-induction decay (FID) were Fourier transformed, which helped to reduce the noise in the final spectra. While analyzing the experimental data, the peak heights were normalized to the adamantane peak at 36.4 ppm within each individual spectrum, and the mass percentage of the sample was also taken into account. At the region of 0-50 ppm, the experimental data was deconvoluted using MestReNova™ (Mestrelab Research) to provide the isolated peak heights for normalization. More details were provided in the previous work [41].

FTIR analysis was performed using a Bruker Vertex 70 spectrometer with a connected Platinum ATR attachment. Samples were scanned 32 times at 2 cm⁻¹ increments using a KBr beam splitter and MCT detector.

3. Results and discussion

In order to study the kinetics of paper waste thermal degradation, it is essential to determine if the temperature of the samples is uniform during the TGA experiments. The following section provides heat transfer modeling of a crucible within the TGA analyzer.

3.1. Heat transfer modeling

In order to determine the heat transfer regime of the system to obtain the temperature transients of the sample during the experiments, Biot Number (Bi) and Thermal Thiele Modulus (M) were

Table 1

Estimated values for the parameters to determine the Bi and M .

Parameter	Value	Source
h , W/m ² -K	10	Free convection
λ for paper waste, W/m-K	0.25	Measured in this study
ρ (apparent), kg/m ³	1200	Measured in this study
c_p (apparent), J/kg-K	1340	[46]
L_c diameter, m	0.0005	Measured in this study

Table 2

M at various temperatures.

Temp (°C)	Rate (s ⁻¹)	R^\dagger (kg/m ³ -s)	M
225	8.6E-06	0.01	1.4×10^{-5}
250	8.6E-05	0.10	1.4×10^{-4}
275	3.9E-04	0.47	6.3×10^{-4}
300	4.0E-04	0.48	6.4×10^{-4}
325	9.0E-04	1.08	1.4×10^{-3}
350	1.3E-03	1.56	2.1×10^{-3}
375	1.5E-03	1.80	2.4×10^{-3}
400	1.6E-03	1.94	2.6×10^{-3}

calculated, which are defined as:

$$Bi = \frac{h}{\lambda/L_c} \quad (1a)$$

$$M = \frac{R^\dagger}{\lambda/(c_p L_c^2)} \quad (2a)$$

Since the paper waste used in this study is a mixture of various paper and cardboard wastes and other materials, it is essential to determine its thermal conductivity. Similar analysis was done for the same experimental setup in our previous study [41]. The parameters used to calculate Bi and M are summarized in Table 1 below.

According to Eq. 1, it was assumed that the h and λ are not dependent on temperature, therefore, Bi was calculated to yield 0.04, which means the heat convection from the oven walls to the sample surface is significantly slower than the heat transfer from the surface into the core of the sample, and the sample temperature is uniform during the experiments.

In order to calculate M , the reaction rates measured at temperature range of 225°C – 400°C are shown in Fig. 1. It shows that the maximum mass loss rate increases as temperatures and at temperature higher than 300°C, the paper waste thermal degradations reach highest rate at around 1,100 s.

From Eq. 2, assuming c_p is also constant, only R^\dagger changes significantly with temperature. Therefore, the highest R^\dagger can yield largest value of M , which is the worst-case scenario. Table 2 shows the maximum reaction rates of the material during experiments determined from Fig. 1, and R^\dagger was calculated by multiplying the maximum reaction rate with the density of the sample (see Table 1). The values of M at different temperatures are also shown in Table 2. As shown in the table, the value of M s vary in the range of 1.4×10^{-5} to 2.6×10^{-3} are significantly smaller than 1. This indicate that reaction rate is dominated by the heat from oven to the sample surface and the sample temperature is uniform and equals to the measured gas temperature.

3.2. Thermal degradation of cellulose, hemicellulose, and lignin

To study the thermal degradation behavior of paper waste, it is essential to analyze the experimental results of cellulose, hemicellulose and lignin degradation. TGA experiments were performed with cellulose, hemicellulose, and lignin individually. Fig. 2 shows the mass loss rates and mass loss versus time of cellulose, hemicellulose and lignin degradation at 325°C and 400°C. The circle

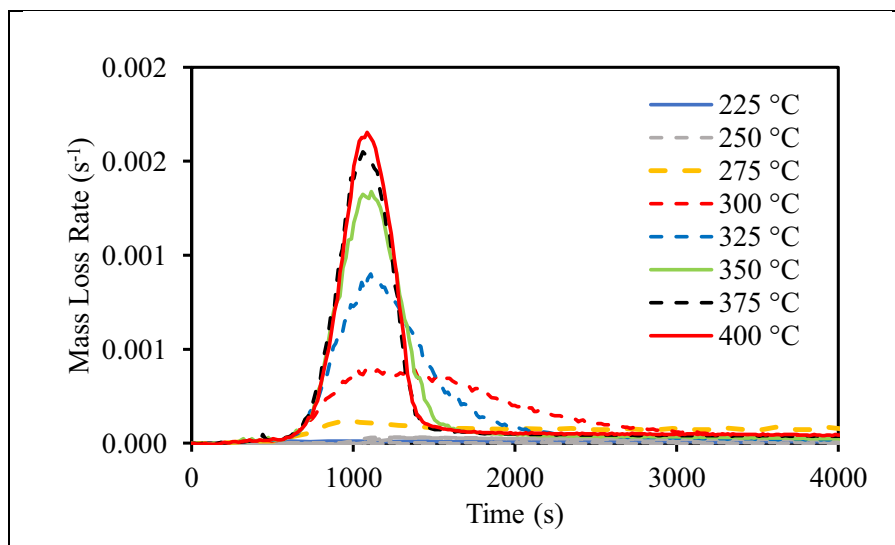


Fig. 1. Measured mass loss rate transient at various temperatures.

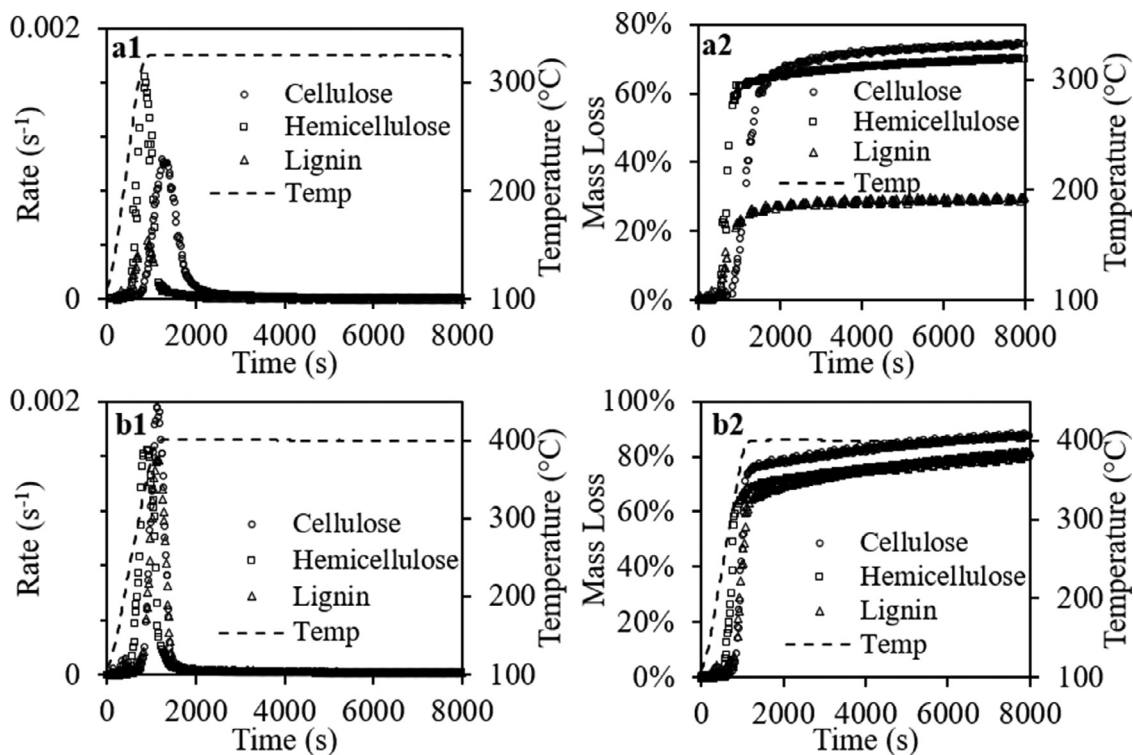


Fig. 2. Mass loss rate of cellulose, hemicellulose and lignin at 325 °C (a1) and 400 °C (b1); mass loss of cellulose, hemicellulose and lignin at 325 °C (a2) and 400 °C (b2).

symbol, square symbol and triangular symbol represent the cellulose, hemicellulose and lignin, respectively. From Fig. 2 (a1), it can be found that at 325 °C, the degradation of hemicellulose started at around 240 °C and the mass loss rate increased rapidly and reached maximum value at around 880 s; the rate of cellulose degradation increased slower but it has a wider time range; the rate of lignin thermal degradation at this temperature is much lower compared to cellulose and hemicellulose. Similar degradation behaviors were also observed in the literature [10,47,48]. Fig. 2 (a2) depicts the mass loss transient of cellulose, hemicellulose and lignin during degradation. Although hemicellulose has higher maximum mass loss rate, the mass loss of cellulose (74.1%) after 8,000 s was slightly higher compared to hemicellulose (70.2%),

and the lignin mass loss at the same time only reached 28.7%. Fig. 2 (b1) shows the temperature transient and the mass loss rate of cellulose, hemicellulose and lignin torrefaction at 400 °C. The degradation of hemicellulose started at around 240 °C and the rate reached peak value at around 375 °C; the degradation of cellulose started at around 275 °C and its highest mass loss rate is slightly higher than hemicellulose; the lignin started degrading at around 350 °C its maximum mass loss rate was very close to hemicellulose. Although hemicellulose started degrading at lower temperature compared to cellulose, its mass loss (81.2%) after 8,000 s was lower than cellulose (87.3%), and the mass loss of lignin after 8,000 s reached 81.1%.

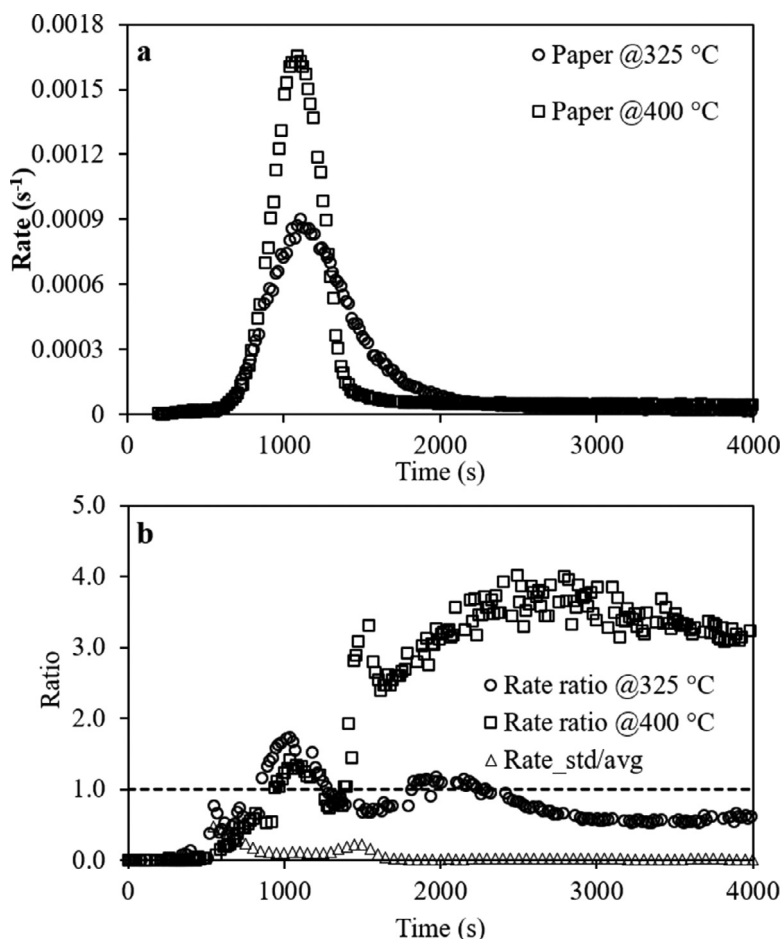


Fig. 3. (a) Experimental results of paper waste mass loss rates @325 and 400°C, and the inset shows the results between 2,000 s and 4,000 s; (b) Rate ratio of experimental results and calculated results @ 325 and 400°C compared to the standard deviation over average values of 19 samples at two temperatures.

Fig. 3a shows the mass loss rate of paper degradation at 325 and 400°C, with the inset showing the rate between 2,000 s and 4,000 s. It can be found that the maximum mass loss rate at 400°C are nearly twice as much as the maximum value at 325°C. The reaction continued at a relatively low rate after 2000 s, with the rate at 400°C also being much higher than the rate at 325°C. The rates of cellulose, hemicellulose and lignin were combined according to the additive law based on their weight composition in the paper waste, and the ratio between the measured experimental results of paper waste degradation and the calculated results assuming no interactions are shown in Fig. 3b. The ratio higher than unity indicates the positive synergies between cellulose, hemicellulose and lignin. To eliminate the impact of the potential experimental uncertainties, the standard deviation of the 19 experimental results at two temperatures over their average values (avg/std) are also added to the plot. The avg/std results indicate the consistency of the experimental results among the 19 samples. In Fig. 3b, for both experiments at 325°C and 400°C, it can be found that there exist some scatters in experimental data before 800 s, after which the results become rather consistent. From Fig. 3b, it can be observed that there are potential interactions for both temperatures at the time range of ~800 s to ~1,400 s, where mass loss rates are very high. After ~1400 s, the results at 400°C also showed potential interactions, with the ratio between the measured results and expected results stayed higher than three.

The ratio between experimental data and expected results that is higher than unity is indicative to potential synergistic effects between cellulose, hemicellulose and lignin. This is an important

finding because it indicates that it is not practical to predict the paper thermal degradation by reconstructing the paper waste thermal degradation model by combining the model of cellulose, hemicellulose and lignin. Therefore, to develop the kinetic model of the paper waste thermal degradation, it is essential to treat paper waste as one material.

3.3. Kinetic modeling

As is mentioned above, paper waste was considered as one material to establish the model for its thermal degradation, a multi-consecutive reaction mechanism was proposed. In addition, according to Klinger et al., more reactions are required as the polymers degrade more completely [38]. Since the TGA only measures the weight of the solids during the experiments, this model focuses on solid products and as follows.



Paper, S_i and k_i denote paper and the solid product of the i^{th} reaction, and the reaction rate of the i^{th} reaction, respectively, and

Carbon is the final product of the thermal degradation of paper waste. The mass loss results were based on dry-ash-free basis, and the number of reactions would differ with different degradation temperatures [23,38]. The reaction rate of all the solids are:

$$\frac{dx_{Paper}}{dt} = -k_1 x_{Paper} \quad (3)$$

$$\frac{dx_{S_{i-1}}}{dt} = \alpha_{i-1} k_{i-1} x_{S_{i-2}} - k_i x_{S_{i-1}} \quad (4)$$

$$\frac{dx_{S_n}}{dt} = \alpha_n k_n x_{S_{n-1}} \quad (5)$$

Where $x_{Paper} = \frac{m_{Paper}}{M_{Paper}}$, $x_{S_i} = \frac{m_{S_i}}{M_{S_i}}$, $\alpha_i = \frac{M_{S_i}}{M_{S_{i-1}}}$.

Assuming the thermal degradation reaction of paper to be first-order and the reaction rate k_i depends on the temperature and follows Arrhenius function:

$$k_i = A_i \exp\left(-\frac{T_{C_i}}{T(t)}\right) \quad (6)$$

Where A_i is the pre-exponential factor and T_{C_i} is the characteristic temperature that equals $\frac{E_{a_i}}{R}$ (E_{a_i} denotes the activation energy of the specific reaction and R is the gas constant). According to the heat transfer model above, the temperature of the sample was uniform and equals to the temperature of the gas. Since the above reaction rate equation only represent the results in molar fraction, while the TGA were measuring the weight of the material, it is essential to transform the above equations into weight fraction.

For Eqs. 3-6, the following can be obtained by multiplying $\frac{m_{S_i}}{m_{Paper}}$:

$$\frac{dy_{Paper}}{dt} = -k_1 y_{Paper} \quad (7)$$

$$\frac{dy_{S_{i-1}}}{dt} = \alpha_{i-1} k_{i-1} y_{S_{i-2}} - k_i y_{S_{i-1}} \quad (8)$$

$$\frac{dy_{S_i}}{dt} = \alpha_i k_i y_{S_{i-1}} \quad (9)$$

Where y_{Paper} and y_{S_i} are the mass fractions of paper and S_i , respectively. By integrating the reaction rate from Eqs. 7-9, the mass fraction of the solids can be obtained, and the mass loss β , can be calculated by:

$$\beta = 1 - (y_{Paper} + y_1 + \dots + y_i) \quad (10)$$

The molar weight ratios between each solid product and initial material can be obtained as follows:

$$\alpha_1 = \frac{M_{S_1}}{M_{Paper}} \quad (11)$$

$$\alpha_1 \alpha_2 \dots \alpha_n = \frac{M_{S_n}}{M_{Paper}} \quad (12)$$

Equation 10 was fitted to the experimental data by adjusting A_i , T_{C_i} and α_i to achieve the best fit with all the results from 225 to 400°C. The fitting was performed through Excel solver add-in function using Generalized Reduced Gradient algorithm. After calculating the summation of error (summation of the square value of the difference between the experimental results and the model results), the summation of errors at each temperature were added together to obtain the total error. The solver function in excel was utilized to achieve the minimum value of the total error by adjusting the kinetic parameters. It was found that it required eight reactions to achieve good fits for the results at 400°C, while it requires less reactions at lower temperatures to achieve good fit. The A_i , T_{C_i} and α_i were kept same for all the temperatures, with some adjustment been made for A_1 at 225, 250 and 275°C to achieve good fit at those three temperatures.

Table 3
Activation energy of each reaction at various temperatures (kJ/mol).

Reaction 1	114.6
Reaction 2	163.8
Reaction 3	160.6
Reaction 4	134.0
Reaction 5	199.5
Reaction 6	185.0
Reaction 7	183.1
Reaction 8	176.6

3.3.1. Modeling at different temperatures

Fig. 4a shows the temperature transients and the mass loss vs. time results at temperatures from 225°C to 400°C, with the black dashed line depicting the temperature transients, red symbol denoting experimental results and the black solid line showing the fitted model. Note that although x-axis was only labeled in the bottom 400°C plot, all of the plots share the same x-axis. The results at 200°C were also carried out but not plotted here since the mass loss was rather insignificant (around 2% after four hours). Fig. 4a showed an excellent fit between the experimental with the model results at various temperatures. The mass loss of paper wastes reached ~4.5% at 225°C after 8,000s, this value increased at the same time to 12.2% at 250°C and 26.7% at 275°C, showing that the extent of paper waste degradation increases with temperature. It was found that there were less reactions required at lower temperatures (3 reactions at 225°C), and the number of equations required increases as the temperature increases. The mass loss increased much faster and reached an asymptotic value of 91.9% at 400°C, and it was found that 8 reactions were needed to achieve a good fit for the experimental results at 400°C.

For Fig. 4b, the black solid line, grey dashed line, orange dashed line, red dashed line, blue dash-dot line, green dash-dot line, blue solid line, orange solid line, and red solid line represent the mass fractions of paper, S_1 , S_2 , S_3 , S_4 , S_5 , S_6 , S_7 and S_8 , respectively. It can be observed that at 225°C, a small fraction of S_1 , S_2 , S_3 were produced and the amount of S_4 to S_8 were negligible after 8,000 s. As temperature increases, more paper waste decomposed and more solid intermediate products were formed. The increase of temperature also increased the rate of paper waste degradation as well as the formation rate of the intermediate solids. At temperatures above 300°C, the mass loss increases rather fast after the reaction started, which can be mainly attributed to the dehydration reaction of cellulose, forming anhydrocellulose [49]. S_5 , represented by the green dash-dot line, started to be produced at 300°C. After temperature went higher, it increased at the beginning and decreased with the extent of thermal decomposition, forming more solid intermediates, with S_6 , observed at 350°C, S_7 found at 375°C, and S_8 only been observed at 400°C.

3.3.2. Model continuity

After obtaining the T_{C_i} for each reaction, the activation energy, E_{a_i} for each reaction was calculated and provided in Table 3.

The activation energy of the first reaction is 114.6 kJ/mol, which is comparable to the results of the activation energy value of cellulose dehydration (106.8 kJ/mol) [50]. The 6th and 7th reactions that appeared at 375°C and 400°C, respectively could be mainly attributed to the degradation of lignin since the maximum degradation of lignin occurs at the temperature range of 375-400°C [51,52]. In addition, the activation energies of these two reactions are around 184 kJ/mol, which was comparable to the literature since lignin has a wide range of activation energy 120.7-197.3 kJ/mol [53]. The reaction at this temperature range is mainly the demethylation of the dimethoxy- groups in lignin, which results in converting phenols into pyrocatechols [10,48].

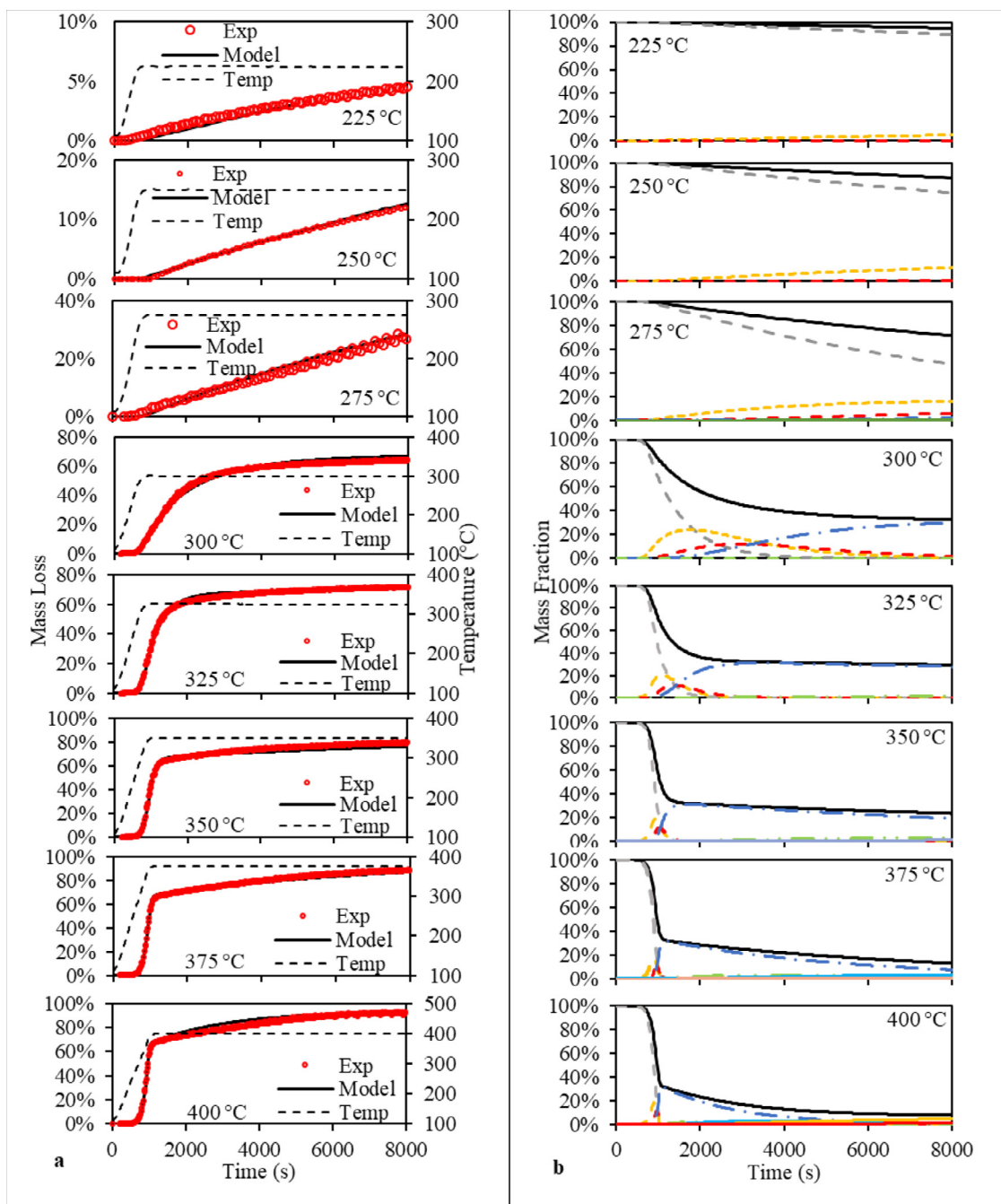


Fig. 4. (a) Temperature transient and mass loss vs. time; (b) mass fractions of paper and solid intermediates vs. time.

3.3.3. Solid product distribution

As mentioned above, the stoichiometric parameters represent the molar weight ratios of the solid products over the reactants. Therefore, with the parameters showed in Table 4, the molar weight of the solid product of each reaction could be obtained.

Fig. 5 shows the molar weight of the solid products of each reaction, the x-axis showing the number of the reactions, with “0” represents the initial paper waste. The initial molar weight of the paper waste was measured to be ~25,800 g/mol. The first degradation reaction could be mainly dehydration and produce solids like anhydrocellulose [49,54]. As the degradation progresses, the molar weight of the solid product reduces and eventually reached 13.6 g/mol, which is very close to carbon (12 g/mol).

Table 4

Molar weight ratios.

Molar weight ratio	Value
α_1	0.51
$\alpha_1\alpha_2$	0.41
$\alpha_1\alpha_2\alpha_3$	0.33
$\alpha_1 \dots \alpha_4$	0.11
$\alpha_1 \dots \alpha_5$	0.09
$\alpha_1 \dots \alpha_6$	0.06
$\alpha_1 \dots \alpha_7$	0.007
$\alpha_1 \dots \alpha_8$	0.001

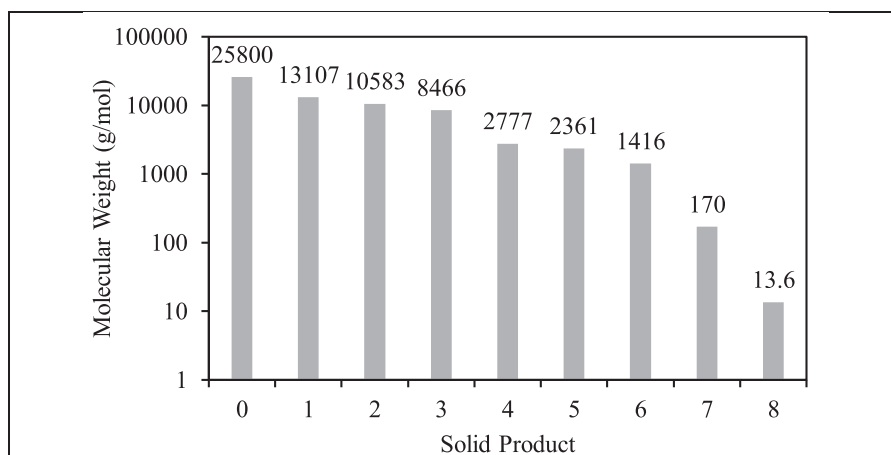


Fig. 5. Molecular weight distribution of solid product after each reaction.

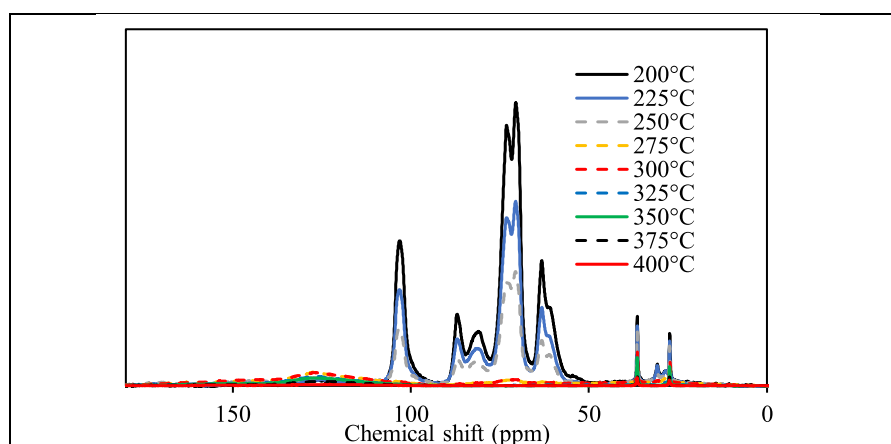


Fig. 6. $^{13}\text{C}[^1\text{H}]$ CP/MAS NMR spectra of torrefied paper residues at temperatures range of 200–400°C.

3.4. NMR spectroscopy

The char residues produced by the TGA experiments were analyzed by NMR spectroscopy to gain further chemical insights and the results are shown in Fig. 6. The peaks between 50 and 100 ppm were identified to be representing the carbons from the cellulosic materials in the paper wastes [55]. It can be observed that as temperatures increases, the peaks at this range decreased in intensity and became insignificant after temperature reached 275°C. At ~127 ppm, a broad peak can be found and were attributed to lignin signals [56]. This phenomenon indicated that some reduction in lignin content with the increase of temperature, but it was less intensive compared to cellulose. This aligns well with the results from literature, showing that the lignin decomposes much slower at lower temperatures[57]. The peak at ~31 ppm was assumed to be waxy aliphatic finish from paper waste, which started to degrade at temperature higher than 250°C. It can also be found that all the above groups were gone in the char product from the 400°C results, indicating that carbon is the final product.

FTIR spectra at varying temperatures show the removal of specific chemical species during the torrefaction process (Fig. 7). The broad peak centered around 3333 cm^{-1} is characteristic of hydrogen bonded -OH present in the cellulose as shown in Fig. 7a. This peak is observed to decrease as temperatures increase, and largely gone at 275°C, similar to what has been observed in the NMR data.

This is likely due to the well-known dehydration reactions that carbohydrates experience through thermochemical conversion and suggested by the kinetic scheme. Additionally, peaks at 1710 and 1600 cm^{-1} , indicative of aromatic lignin, begin to be more prevalent in the IR spectra as cellulose is removed. These peaks begin to disappear at 325°C and are almost entire gone at 400°C. The peak at 1419 cm^{-1} is consistent with the C-H₂ bending mode, but is also present at temperatures above 350°C. Calcium carbonate also has a strong peak at 1420 cm^{-1} , which likely accounts for the peak persisting, as C-H₂ is removed CaCO₃ is generated maintaining that same peak. Calcium and silicon compounds are often used in pigments and coatings on papers to enhance the end-use properties and are expected in real wastepaper streams. Peaks at 872 and 713 cm^{-1} can be observed at higher temperatures, which are also associated with CaCO₃.

Another significant peak at lower temperatures is observed at 1158 cm^{-1} , which is associated with C-O-C in cellulose (Fig. 7b). This peak disappears as temperature increases and cellulose is removed, revealing peaks at 1033 and 1008 cm^{-1} . These peaks at 1033 and 1008 cm^{-1} are Si-O stretching modes, which persist as temperature increases. All of these identifications are consistent with the predicted cellulose degradation, followed by small contributions from the lignin content. Both spectroscopic techniques presented on the intermediate char species corroborate the kinetic scheme and validate the assumptions and approach.

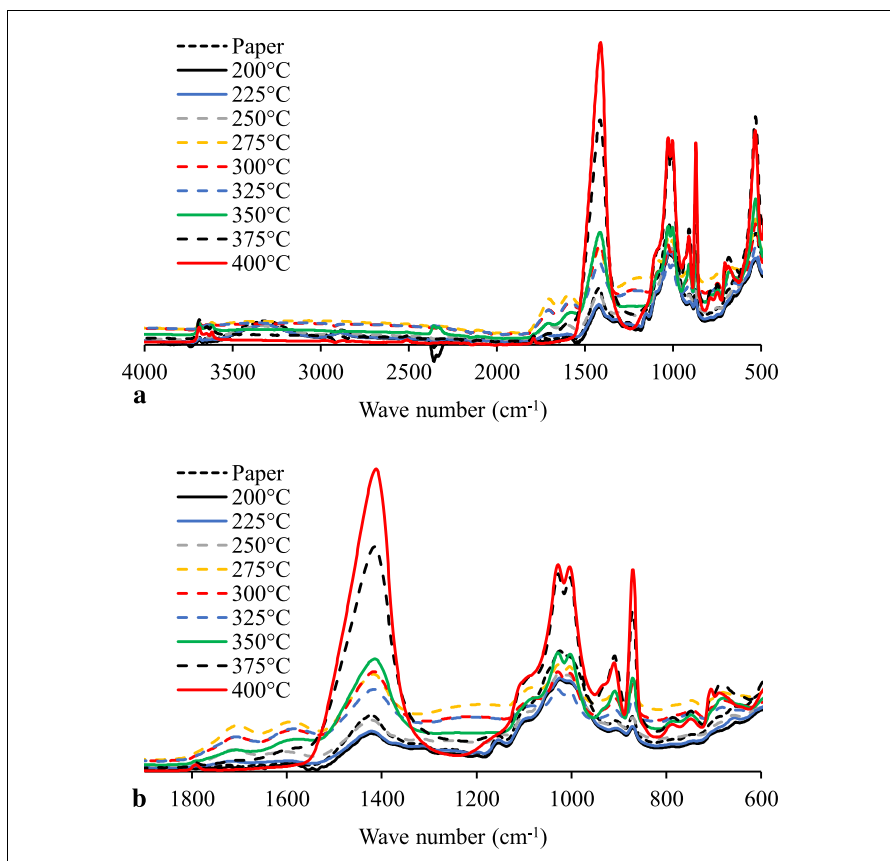


Fig. 7. FTIR spectra of torrefied paper samples at various temperatures: (a) full spectra of wave number from 500–4000 cm^{-1} ; spectra of wave number from 600–1900 cm^{-1} .

4. Conclusions

Thermal degradation of paper waste was studied through thermogravimetric analysis at the temperature range of 200–400°C. Two kinetic approaches were taken to develop the kinetic model for paper waste degradation: (i) reconstructing the TGA results of paper waste thermal degradation by an additive law of the degradation of cellulose, hemicellulose and lignin; (ii) considering paper waste as one material and develop a multi-step consecutive reaction mechanism that focuses on solid products at different temperatures. It was found that there exists potential synergistic effects between cellulose, hemicellulose and lignin during paper waste degradation. Therefore, this study took the second approach. The temperature transients were modeled, and one set of kinetic parameters were obtained through fitting to the TGA experimental results. The model showed: (i) the first reaction was mainly dehydration reaction of cellulose with anhydrocellulose as solid product; (ii) there are more reactions at higher temperatures; (iii) the activation energies of 6th and 7th reaction and the temperatures (375°C and 400°C) are comparable to the results of lignin thermal degradation in literature, thus can be attributed lignin thermal degradation. The NMR and FTIR results also indicated that the cellulose started degrading at lower temperatures, followed by small contributions from lignin. And lignin degradation became more pronounced at higher temperatures. This model can not only provide chemical insights of the paper wastes thermal degradation, it also can be used to help with other mechanistic works.

Authors statement

Xu: Methodology, Investigation and Writing Original Draft; Kolapkar: Investigation and Writing Review and Editing; Zinchik: In-

vestigation and Writing Review and Editing; Fillerup: Investigation and Investigation and Writing Review and Editing Schaller; Investigation and Writing Review and Editing; Bar-Ziv: Conceptualization and Supervision; Klinger: Supervision and Investigation.

Declaration of competing interest

The authors do not have any competing interest.

Acknowledgements

We acknowledge the guidance on the data fitting process from Dr. Victor M Zavala; and the support from (1) National Science Foundation grant number 1827364; and (2) supported by the U.S. Department of Energy (DOE), Office of Energy Efficiency and Renewable Energy (EERE), Bioenergy Technologies Office (BETO), under DOE Idaho Operations Office Contract DE-AC07-05ID14517.

References

- [1] Paper and Paperboard: Material-Specific Data | Facts and Figs. about Materials, Waste and Recycling, US EPA, 2018 <https://www.epa.gov/facts-and-figures-about-materials-waste-and-recycling/paper-and-paperboard-material-specific-data> accessed July 28, 2020.
- [2] J.G. McCabe, Addressing Biogenic Carbon Dioxide Emissions from Stationary Sources, United States Environmental Protection Agency, Washington, D.C, 2014 <https://archive.epa.gov/epa/sites/production/files/2016-08/documents/biogenic-co2-emissions-memo-111914.pdf>.
- [3] S.J. Eichhorn, J. Sirichaisit, R.J. Young, Deformation mechanisms in cellulose fibres, paper and wood, *J. Mater. Sci.* 36 (2001) 3129–3135, doi:10.1023/A:1017969916020.
- [4] Y. Ma, M. Hummel, M. Määttänen, A. Särkilähti, A. Harlin, H. Sixta, Upcycling of waste paper and cardboard to textiles, *Green Chem* 18 (2016) 858–866, doi:10.1039/c5gc01679g.

- [5] A.G.W. Bradbury, Y. Sakai, F. Shafizadeh, A kinetic model for pyrolysis of cellulose, *J. Appl. Polym. Sci.* 23 (1979) 3271–3280, doi:[10.1002/app.1979.070231112](https://doi.org/10.1002/app.1979.070231112).
- [6] L. Cabrales, N. Abidi, On the thermal degradation of cellulose in cotton fibers, *J. Therm Anal Calorim* 102 (2010) 485–491, doi:[10.1007/s10973-010-0911-9](https://doi.org/10.1007/s10973-010-0911-9).
- [7] V. Mamleev, S. Bourbigot, J. Yvon, Kinetic analysis of the thermal decomposition of cellulose: The main step of mass loss, *J. Anal. Appl. Pyrolysis*. 80 (2007) 151–165, doi:[10.1016/j.jaap.2007.01.013](https://doi.org/10.1016/j.jaap.2007.01.013).
- [8] D.K. Shen, S. Gu, A.V. Bridgwater, Study on the pyrolytic behaviour of xylan-based hemicellulose using TG-FTIR and Py-GC-FTIR, *J. Anal. Appl. Pyrolysis*. 87 (2010) 199–206, doi:[10.1016/j.jaap.2009.12.001](https://doi.org/10.1016/j.jaap.2009.12.001).
- [9] F.X. Collard, J. Blin, A review on pyrolysis of biomass constituents: Mechanisms and composition of the products obtained from the conversion of cellulose, hemicelluloses and lignin, *Renew. Sustain. Energy Rev.* 38 (2014) 594–608, doi:[10.1016/j.rser.2014.06.013](https://doi.org/10.1016/j.rser.2014.06.013).
- [10] M. Brebu, C. Vasile, Thermal Degradation of Lignin-A Review, *Cellul. Chem. Technol.* 44 (2010) 353–363 <https://www.semanticscholar.org/paper/THERMAL-DEGRADATION-OF-LIGNIN-A-REVIEW-Brebu-Vasile/67f6cc0d827e7ac1cbb5a4c6752b6d8ec6c1fef>, accessed August 7, 2020.
- [11] R. Alén, E. Kuoppala, P. Oesch, Formation of the main degradation compound groups from wood and its components during pyrolysis, *J. Anal. Appl. Pyrolysis*. 36 (1996) 137–148, doi:[10.1016/0165-2370\(96\)00932-1](https://doi.org/10.1016/0165-2370(96)00932-1).
- [12] J. Rodrigues, J. Graça, H. Pereira, Influence of tree eccentric growth on syringyl/guaiacyl ratio in Eucalyptus globulus wood lignin assessed by analytical pyrolysis, *J. Anal. Appl. Pyrolysis*. 58–59 (2001) 481–489, doi:[10.1016/S0165-2370\(00\)00121-2](https://doi.org/10.1016/S0165-2370(00)00121-2).
- [13] K. Raveendran, Pyrolysis characteristics of biomass and biomass components, *Fuel*. 75 (1996) 987–998. [https://doi.org/10.1016/0016-2361\(96\)00030-0](https://doi.org/10.1016/0016-2361(96)00030-0).
- [14] H. Yang, R. Yan, H. Chen, C. Zheng, D.H. Lee, V. Uni, N.D. V. R.V. March, V. Re, M. Recci, V. September, In-Depth Investigation of Biomass Pyrolysis Based on Three Major Components: Hemicellulose, Cellulose and Lignin, (2006) 388–393. <https://doi.org/10.1021/ef0580117>.
- [15] E. Biagini, F. Barontini, L. Tognotti, V. Diotisal, Devolatilization of Biomass Fuels and Biomass Components Studied by TG /FTIR Technique, (2006) 4486–4493. <https://doi.org/10.1021/ie0514049>.
- [16] S. Zhao, M. Liu, L. Zhao, L. Zhu, Influence of Interactions among Three Biomass Components on the Pyrolysis Behavior, *Ind. Eng. Chem. Res.* 57 (2018) 5241–5249. <https://doi.org/10.1021/acs.iecr.8b00593>.
- [17] S. Wu, D. Shen, J. Hu, H. Zhang, R. Xiao, Biomass and Bioenergy Cellulose-lignin interactions during fast pyrolysis with different temperatures and mixing methods, 90 (2016). <https://doi.org/10.1016/j.biombioe.2016.04.012>.
- [18] T.J. Hilbers, Z. Wang, B. Pecha, R.J.M. Westerhof, S.R.A. Kersten, M.R. Pelaez-samaniego, M. Garcia-perez, Cellulose-Lignin interactions during slow and fast pyrolysis, *J. Anal. Appl. Pyrolysis*. 114 (2015) 197–207, doi:[10.1016/j.jaap.2015.05.020](https://doi.org/10.1016/j.jaap.2015.05.020).
- [19] R. Volpe, A.A. Zabaniotou, V. Skoulou, Synergistic Effects between Lignin and Cellulose during Pyrolysis of Agricultural Waste, (2018). <https://doi.org/10.1021/acs.energyfuels.8b00767>.
- [20] J. Zhang, Y.S. Choi, C.G. Yoo, T.H. Kim, R.C. Brown, B.H. Shanks, Cellulose–Hemicellulose and Cellulose–Lignin Interactions during Fast Pyrolysis, *ACS Sustain. Chem. Eng.* 3 (2015) 293–301. <https://doi.org/10.1021/sc500664h>.
- [21] H. Yang, M. Liu, Y. Chen, S. Xin, X. Zhang, X. Wang, H. Chen, Vapor – solid interaction among cellulose, hemicellulose and lignin, *Fuel* 263 (2020), doi:[10.1016/j.fuel.2019.116681](https://doi.org/10.1016/j.fuel.2019.116681).
- [22] J. Klinger, E. Bar-Ziv, D. Shonnard, Kinetic study of aspen during torrefaction, *J. Anal. Appl. Pyrolysis*. 104 (2013) 146–152, doi:[10.1016/j.jaap.2013.08.010](https://doi.org/10.1016/j.jaap.2013.08.010).
- [23] J. Klinger, B. Klemetsrud, E. Bar-Ziv, D. Shonnard, Temperature dependence of aspen torrefaction kinetics, *J. Anal. Appl. Pyrolysis*. 110 (2014) 424–429, doi:[10.1016/j.jaap.2014.10.008](https://doi.org/10.1016/j.jaap.2014.10.008).
- [24] G. Várhegyi, M.J. Antal, E. Jakab, P. Szabó, Kinetic modeling of biomass pyrolysis, *J. Anal. Appl. Pyrolysis*. 42 (1997) 73–87, doi:[10.1016/S0165-2370\(96\)00971-0](https://doi.org/10.1016/S0165-2370(96)00971-0).
- [25] H. Zhou, Y. Long, A. Meng, S. Chen, Q. Li, Y. Zhang, A novel method for kinetics analysis of pyrolysis of hemicellulose, cellulose, and lignin in TGA and macro-TGA, *RSC Adv* 5 (2015) 26509–26516, doi:[10.1039/c5ra02715b](https://doi.org/10.1039/c5ra02715b).
- [26] V. Pasangulapati, K.D. Ramachandriya, A. Kumar, M.R. Wilkins, C.L. Jones, R.L. Huhnke, Effects of cellulose, hemicellulose and lignin on thermochemical conversion characteristics of the selected biomass, *Bioresour. Technol.* 114 (2012) 663–669, doi:[10.1016/j.biortech.2012.03.036](https://doi.org/10.1016/j.biortech.2012.03.036).
- [27] M.A. Hubbe, R.A. Venditti, O.J. Rojas, What happens to cellulosic fibers during papermaking and recycling? A review, *BioResources*. 2 (2007) 739–788. <https://doi.org/10.15376/biores.2.4.739-788>.
- [28] W. Farhat, R. Venditti, A. Quick, M. Taha, N. Mignard, F. Becquart, A. Ayoub, Hemicellulose extraction and characterization for applications in paper coatings and adhesives, *Ind. Crop. Prod.* 107 (2017) 370–377, doi:[10.1016/j.indcrop.2017.05.055](https://doi.org/10.1016/j.indcrop.2017.05.055).
- [29] V. Repellin, A. Govin, M. Rolland, R. Guyonnet, Modelling anhydrous weight loss of wood chips during torrefaction in a pilot kiln, *Biomass and Bioenergy* 34 (2010) 602–609, doi:[10.1016/j.biombioe.2010.01.002](https://doi.org/10.1016/j.biombioe.2010.01.002).
- [30] C. Branca, A. Albano, C. Di Blasi, Critical evaluation of global mechanisms of wood devolatilization, *Thermochim. Acta.* 429 (2005) 133–141, doi:[10.1016/j.tca.2005.02.030](https://doi.org/10.1016/j.tca.2005.02.030).
- [31] M. Broström, A. Nordin, L. Pommer, C. Branca, C. Di Blasi, Influence of torrefaction on the devolatilization and oxidation kinetics of wood, *J. Anal. Appl. Pyrolysis*. 96 (2012) 100–109, doi:[10.1016/j.jaap.2012.03.011](https://doi.org/10.1016/j.jaap.2012.03.011).
- [32] J.J. Manyà, E. Velo, L. Puigjaner, Kinetics of biomass pyrolysis: A reformulated three-parallel-reactions model, *Ind. Eng. Chem. Res.* 42 (2003) 434–441, doi:[10.1021/ie020218p](https://doi.org/10.1021/ie020218p).
- [33] M.J. Prins, K.J. Ptasinski, F.J.J.G. Janssen, Torrefaction of wood. Part 1. Weight loss kinetics, *J. Anal. Appl. Pyrolysis*. 77 (2006) 28–34, doi:[10.1016/j.jaap.2006.01.002](https://doi.org/10.1016/j.jaap.2006.01.002).
- [34] H. Chen, N. Liu, W. Fan, Two-step Consecutive Reaction Model of Biomass Thermal Decomposition by DSC, *Acta Phys. - Chim. Sin.* 22 (2006) 786–790, doi:[10.1016/S1872-1508\(06\)60031-4](https://doi.org/10.1016/S1872-1508(06)60031-4).
- [35] H. Chen, N. Liu, W. Fan, Two-Step consecutive reaction model and kinetic parameters relevant to the decomposition of Chinese forest fuels, *J. Appl. Polym. Sci.* 102 (2006) 571–576, doi:[10.1002/app.24310](https://doi.org/10.1002/app.24310).
- [36] J. Klinger, E. Bar-Ziv, D. Shonnard, Predicting properties of torrefied biomass by intrinsic kinetics, *Energy and Fuels* 29 (2015) 171–176, doi:[10.1021/ef501456p](https://doi.org/10.1021/ef501456p).
- [37] J. Klinger, E. Bar-ziv, D. Shonnard, T. Westover, R. Emerson, Predicting Properties of Gas and Solid Streams by Intrinsic Kinetics of Fast Pyrolysis of Wood, (2016). <https://doi.org/10.1021/acs.energyfuels.5b01877>.
- [38] J. Klinger, E. Bar-Ziv, D. Shonnard, Unified kinetic model for torrefaction-pyrolysis, *Fuel Process. Technol.* 138 (2015) 175–183, doi:[10.1016/j.fuproc.2015.05.010](https://doi.org/10.1016/j.fuproc.2015.05.010).
- [39] Z. Xu, S. Zinchik, S. Kolapkar, E. Bar-ziv, T. Hansen, D. Conn, Properties of Torrefied U.S. Waste Blends, *Front. Energy Res.* 6 (2018) 65, doi:[10.3389/fenrg.2018.00065](https://doi.org/10.3389/fenrg.2018.00065).
- [40] Z. Xu, J.W. Albrecht, S.S. Kolapkar, S. Zinchik, E. Bar-Ziv, Chlorine Removal from U.S. Solid Waste Blends through Torrefaction, *Appl. Sci.* 10 (2020) 3337, doi:[10.3390/app1009337](https://doi.org/10.3390/app1009337).
- [41] Z. Xu, S.S. Kolapkar, S. Zinchik, E. Bar-Ziv, L. Ewurum, A.G. McDonlad, J.L. Klinger, E. Fillerup, K. Schaller, C. Pilgrim, Bypassing Energy Barriers in Fiber-Polymer Torrefaction, *Front. Energy Res.* 9 (2021) 75, doi:[10.3389/FENRG.2021.643371](https://doi.org/10.3389/FENRG.2021.643371).
- [42] S.N. Patkar, P.D. Panzade, Fast and efficient method for molecular weight analysis of cellulose pulp, in-process and finished product, *Anal. Methods*. 8 (2016) 3210–3215, doi:[10.1039/c5ay03012a](https://doi.org/10.1039/c5ay03012a).
- [43] A. Pines, M.G. Gibby, J.S. Waugh, Proton-enhanced nuclear induction spectroscopy: a method for high resolution nmr of dilute spins in solids, *J. Chem. Phys.* 56 (1972) 1776–1777, doi:[10.1063/1.1677439](https://doi.org/10.1063/1.1677439).
- [44] J. Schaefer, E.O. Stejskal, R. Buchdahl, High-Resolution Carbon-13 Nuclear Magnetic Resonance Study of Some Solid, Glassy Polymers, *Macromolecules* 8 (1975) 291–296, doi:[10.1021/ma60045a010](https://doi.org/10.1021/ma60045a010).
- [45] B.M. Fung, A.K. Khitrin, K. Ermolaev, An Improved Broadband Decoupling Sequence for Liquid Crystals and Solids, *J. Magn. Reson.* 142 (2000) 97–101, doi:[10.1006/jmre.1999.1896](https://doi.org/10.1006/jmre.1999.1896).
- [46] A.Mahdavi Nejad, Thermal Analysis of Paper Board Packaging with Phase Change Material: A Numerical Study, *J. Packag. Technol. Res.* 3 (2019) 181–192, doi:[10.1007/s41783-019-00060-1](https://doi.org/10.1007/s41783-019-00060-1).
- [47] J.Y. Yeo, B.L.F. Chin, J.K. Tan, Y.S. Loh, Comparative studies on the pyrolysis of cellulose, hemicellulose, and lignin based on combined kinetics, *J. Energy Inst.* 92 (2019) 27–37, doi:[10.1016/j.joei.2017.12.003](https://doi.org/10.1016/j.joei.2017.12.003).
- [48] W.H. Chen, C.W. Wang, H.C. Ong, P.L. Show, T.H. Hsieh, Torrefaction, pyrolysis and two-stage thermodegradation of hemicellulose, cellulose and lignin, *Fuel* 258 (2019) 116–168, doi:[10.1016/j.fuel.2019.116168](https://doi.org/10.1016/j.fuel.2019.116168).
- [49] J. Scheirs, G. Camino, W. Tumiatti, Overview of water evolution during the thermal degradation of cellulose, *Eur. Polym. J.* 37 (2001) 933–942, doi:[10.1016/S0014-3057\(00\)00211-1](https://doi.org/10.1016/S0014-3057(00)00211-1).
- [50] V.A. Alvarez, A. Vázquez, Thermal degradation of cellulose derivatives/starch blends and sisal fibre biocomposites, *Polym. Degrad. Stab.* 84 (2004) 13–21, doi:[10.1016/j.polyimdegradstab.2003.09.003](https://doi.org/10.1016/j.polyimdegradstab.2003.09.003).
- [51] M. Brebu, T. Tamminen, I. Spiridon, Thermal degradation of various lignins by TG-MS/FTIR and Py-GC-MS, *J. Anal. Appl. Pyrolysis*. 104 (2013) 531–539, doi:[10.1016/j.jaap.2013.05.016](https://doi.org/10.1016/j.jaap.2013.05.016).
- [52] J. Zhao, W. Xiuwen, J. Hu, Q. Liu, D. Shen, R. Xiao, Thermal degradation of softwood lignin and hardwood lignin by TG-FTIR and Py-GC/MS, *Polym. Degrad. Stab.* 108 (2014) 133–138, doi:[10.1016/j.polyimdegradstab.2014.06.006](https://doi.org/10.1016/j.polyimdegradstab.2014.06.006).
- [53] A. Ház, M. Jablonský, I. Šurina, F. Kačík, T. Bubeníková, J. Đurkovič, Chemical composition and thermal behavior of kraft lignins, *Forests*. 10 (2019) 1–12. <https://doi.org/10.3390/f10060483>.
- [54] Y. Sekiguchi, J.S. Frye, F. Shafizadeh, Structure and formation of cellulosic chars, *J. Appl. Polym. Sci.* 28 (1983) 3513–3525, doi:[10.1002/app.1983.070281116](https://doi.org/10.1002/app.1983.070281116).
- [55] S.L. Maunu, 13C CPMAS NMR Studies of Wood, Cellulose Fibers, and Derivatives, in: Q. Thomas, Q. Hu (Eds.), *Charact. Lignocellul. Mater.*, Blackwell, Hoboken, 2009: pp. 227–248. <https://doi.org/https://doi.org/10.1002/9781444305425.ch13>.
- [56] D. Lauer, E.L. Motell, D.D. Traficante, G.E. Maciel, Carbon-13 Chemical Shifts in Monoalkyl Benzenes and Some Deuterio Analogs, *J. Am. Chem. Soc.* 94 (1972) 5335–5338, doi:[10.1021/ja00770a032](https://doi.org/10.1021/ja00770a032).
- [57] J. Hu, D. Shen, S. Wu, H. Zhang, R. Xiao, Effect of temperature on structure evolution in char from hydrothermal degradation of lignin, *J. Anal. Appl. Pyrolysis*. 106 (2014) 118–124, doi:[10.1016/j.jaap.2014.01.008](https://doi.org/10.1016/j.jaap.2014.01.008).